ELSEVIER

Journal of Chromatography A, 872 (2000) 23–35

JOURNAL OF CHROMATOGRAPHY A

www.elsevier.com/locate/chroma

Design of a simulated moving bed unit for sucrose–betaine separations☆

Sergio Giacobello, Giuseppe Storti, Giuseppe Tola*

Dipartimento di Ingegneria Chimica e Materiali, University of Cagliari, Piazza d'Armi, 09123 Cagliari, Italy

Received 27 July 1999; received in revised form 11 November 1999; accepted 3 December 1999

Abstract

The results of a series of pulse experiments carried out in a fixed bed column packed with a strongly acid ion-exchange resin and with reference to the separation of an aqueous sucrose–betaine mixture are presented. These data were used to evaluate equilibrium and diffusion parameters for both key components in the frame of linear chromatography theory. The estimated values were used to design a simulated moving bed plant aimed to separate betaine from sucrose in beet molasses.
© 2000 Published by Elsevier Science B.V. All rights reserved.

Keywords: Simulated moving bed chromatography; Preparative chromatography; Instrumentation; Sucrose; Betaine; Sugars

1. Introduction

The production of sucrose in beetsugar factories leads to large volumes of molasses, frequently sold off as animal feed. Molasses is the final syrup obtained after repeated crystallisation steps. To improve the process economy, the desugarization of molasses with recovery of dissolved sugar and of valuable products of nonsugar fraction is gaining increasing importance [1,2]. Among these, betaine is one of the most interesting compounds [3,4], usually present in concentrations between 4 and 7% (w/w).

Most of the industrial applications and experimental studies performed in the field of molasses treatment are focused on the separation between sugars and nonsugars or on the subsequent separation of glucose–fructose from the sugar fraction [5–7]. For these separations, a simulated moving bed (SMB) adsorber operating in the liquid phase is a common process choice [2,8].

For a reliable modelling and design of the separation unit at the industrial scale, the essential parameters are those characterising adsorption equilibrium and mass transfer efficiency for the key components [9]. When dealing with the simplest case of linear equilibria, experimental pulse tests on a laboratory column combined with the linear chromatography theory [10] is an effective approach to their evaluation.

In this paper, experimental results obtained for the adsorption separation of an aqueous sucrose–betaine mixture on a laboratory scale, fixed-bed column packed with an ion-exchange resin are presented. These data were used to evaluate equilibrium and diffusion parameters for both key components in the frame of linear chromatography theory. Finally, these

☆Presented at the 1999 International Symposium on Preparative/Process Chromatography, San Francisco, CA, 23–26 May 1999.

*Corresponding author.

0021-9673/00/$ – see front matter © 2000 Published by Elsevier Science B.V. All rights reserved.
PII: S0021-9673(99)01289-3

values are used to make a preliminary design of a SMB unit aimed to separate betaine from sucrose in beet molasses.

2. Experimental

The experimental apparatus is schematically shown in Fig. 1. A piston pump (3; Model RH/0C KC, Fluid Metering, New York, NY, USA) was used to flow eluent (reservoir 1) and adsorbable components through the column (6). To bypass the column, two three-way valves (5) were installed. The injection of the pulse was performed through the six-way valve (4), whose loop volume was 6.15 cm^3. The column (plexiglass tube of 37.1 cm×1.6 cm I.D.) was thermostatted by flowing through the jacket water from a thermostatic bath (2). The column was packed with a strongly acid ion-exchange resin (Dowex 50 W-X8-400, K^+ form; Sigma, St. Louis, MO, USA) with average particle diameter about 56 μm. The stream eluted from the column was directly sent to a refractive index (RI) detector (Model 1047A, Hewlett-Packard, Palo Alto, CA, USA). Data acquisition was performed with a personal computer, using the software ChromCard (Carlo Erba, Milan, Italy).

The experiments were carried out following two different operating modes, pulse and frontal. In the first case, a pulse of an aqueous solution of each component was fed to the column through the loop of the six-way valve. In the second case, the same solution was continuously fed from the reservoir (1).

Since this work is focused on application to beet molasses, a model mixture involving selected key components in water was identified. The typical composition of a European beet molasses is the following (%, w/w): sugars=47.6–52.1; organic non-sugars=14.5–18.0 (with a betaine content from 4.0 to 7.0); inorganic non-sugars=6.4–6.8 (with a KCl content from 3.2 to 4.8). Accordingly, the following composition of the model mixture was defined (%, w/w): sucrose=50; betaine=20; KCl=10. Thus, the chemicals used in the experimental runs were sucrose (ACS grade, Aldrich, Milwaukee, WI, USA), betaine (98%, Aldrich) and KCl (RPE-ACS grade, Carlo Erba). All pulse experiments discussed below were carried out using monocomponent aqueous solutions of each key component with concentration scaled to those of the model solution. This means that, given a certain pulse concentration of sucrose (namely, 0.5, 1.0 and 2.0 g dm^{-3}), the corresponding values for betaine and KCl were selected to fulfil a ratio to sucrose 2:5 and 1:5, respectively. The following values of liquid flow-rate, Q, and temperature, T, were examined: Q=0.5, 1.0, 1.5 cm^3 min^{-1}, T=25, 40, 60°C. The external void ratio of the column, ϵ=0.4, was estimated by

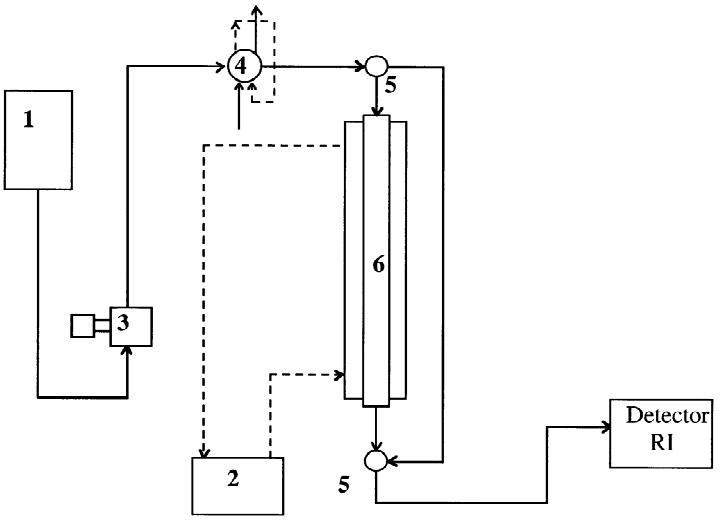

Fig. 1. Schematic representation of the experimental apparatus.

pulse experiments using blue dextran as inert compound.

3. Data reduction

The evaluation of equilibrium constants and column efficiencies was performed using the linear chromatographic theory [10,11]. Accordingly, first moment, μ_1, and variance, σ^2, of the eluted concentration peak were estimated by numerical integration and expressed in terms of the target quantities through the following equations:

$$\mu_1 = \frac{L}{v} \cdot \left(1 + \frac{1-\epsilon}{\epsilon} \cdot K_i\right) \tag{1}$$

$$\sigma^2 = \frac{2LD_L}{v^3} \cdot \left(1 + K_i'^2\right)^2 + 2 \cdot \frac{L}{v} \cdot \frac{\epsilon K_i'^2}{1-\epsilon} \cdot t_{mi} \tag{2}$$

where v indicates the interstitial velocity of the fluid phase, L the column length, K_i the equilibrium constant of adsorption, D_L the axial mixing coefficient, t_{mi} a characteristic time of diffusion of component i in the resin particle and K_i' a capacity factor, defined as $K_i(1-\epsilon)/\epsilon$.

The adsorptivity of each component, K_i, is readily estimated through the first equation above. Moreover, the linearity of the adsorption equilibria can be checked by pulse experiments at different concentrations: constant K_i values have to be obtained in all runs. About the transport phenomena, the second equation is usually recast in terms of the height equivalent to a theoretical plate, HETP, as follows:

$$\mathrm{HETP}_i = \frac{2D_L}{v} + \frac{2v\epsilon}{1-\epsilon} \cdot \left(\frac{K_i'}{1+K_i'}\right)^2 \cdot t_{mi} \tag{3}$$

which is the well-known Van Deemter equation [12]. Two contributions to the column efficiency can be identified, the one related to fluid dynamics non idealities and the other to the intraparticle transport phenomena, lumped in the time parameter t_{mi}. Its actual expression is determined by the assumed particle morphology. In the case of gel-type ion-exchange resins, two diffusive steps are usually identified, transport through the external fluid film and diffusion through the polymeric matrix in the adsorbed phase. If the second step is rate determining (as found in most of the practical cases), the following expression for t_{mi} applies:

$$t_{mi} = \frac{r_p^2}{15 D_{si} K_i} \tag{4}$$

where r_p indicates the particle radius and D_{si} the diffusion coefficient of component i inside the polymer matrix. By performing chromatographic experiments at different flow-rates, HETP_i values are measured and plotted as a function of the fluid velocity. Since typical relationships to evaluate the axial mixing coefficient for liquid in packed beds [13] indicate a linear dependence of D_L upon the fluid velocity in the range of flow-rates under examination, Eq. (3) can be further reduced to the simple form:

$$\mathrm{HETP}_i = a_i r_p + b_i r_p^2 v \tag{5}$$

where a_i and b_i are defined as follows:

$$a_i = \frac{2D_L}{v r_p}; \quad b_i = \frac{2\epsilon}{1-\epsilon} \cdot \left(\frac{K_i'}{1+K_i'}\right)^2 \cdot \frac{1}{15 D_{si} K_i} \tag{6}$$

thus accounting for axial mixing and intraparticle transport resistances, respectively.

Finally, it is worth mentioning that the peak moments which are referred to in Eqs. (1) and (2) have to account for the effects of the chromatographic column only. However, the actual experimental data are affected by extracolumn parts of the unit, such as injector, tubing, valves and detector. In the linear chromatography theory [10] the resulting moments are expressed assuming the superposition of these effects and the corrected values of the moments to be used in Eqs. (1) and (2) are evaluated as:

$$\mu_{1i} = \mu_{1i,\,\mathrm{exp}} - \mu_{1i,\,\mathrm{extra}} \tag{7}$$

$$\sigma_i^2 = \sigma_{i,\,\mathrm{exp}}^2 - \sigma_{i,\,\mathrm{extra}}^2 \tag{8}$$

The values of the extracolumn moments were estimated by pulse experiments completely equivalent to those described above but without the col-

Table 1
Equilibrium constant values for KCl at different flow-rates and pulse concentrations

K	Q (cm^3 min^{-1})	c (g dm^{-3})	T (°C)
0.025	1.042	0.10	25
0.020	1.048	0.26	25
0.022	1.052	0.44	25

umn, i.e., bypassing it using the three-way valves shown in Fig. 1.

3.1. Equilibrium constants

The estimated values of the equilibrium constants K_i are summarised in Tables 1–3 for KCl, sucrose and betaine, respectively, along with the corresponding operating conditions (temperature, flow-rate and concentration). The values indicate linear equilibrium conditions for both KCl and sucrose (reasonably constant values were obtained when considering runs at the same temperature) but not for betaine. In the KCl case, the adsorptivity is very small and indicates that the retention of the salt can be neglected with respect to that of the other components. Moreover, the expected decrease of K_i with the temperature increase was always verified.

Table 2
Equilibrium constant values for sucrose at different flow-rates, pulse concentrations and temperatures

K	Q (cm^3 min^{-1})	c (g dm^{-3})	T (°C)
0.168	1.00	0.59	25
0.162	1.05	1.04	25
0.167	1.00	2.02	25
0.160	0.51	1.04	25
0.162	1.05	1.04	25
0.164	1.56	1.04	25
0.138	1.06	1.06	40
0.136	1.05	1.06	60

Table 3
Equilibrium constant values for betaine at different flow-rates, pulse concentrations and temperatures

K	Q (cm^3 min^{-1})	c (g dm^{-3})	T (°C)
0.696	1.00	0.21	25
0.641	0.92	0.41	25
0.635	1.00	0.81	25
0.646	0.52	0.41	25
0.641	1.04	0.41	25
0.648	1.57	0.41	25
0.612	1.06	0.40	40
0.599	1.05	0.40	60

To identify a possible concentration dependence of the equilibrium constant of the betaine, additional experiments were carried out using a different operating mode. Namely, a constant concentration step was fed to the column and maintained up to the equilibration of the whole resin (frontal mode). From the eluted concentration profile, the solid-phase concentration in equilibrium with the fluid phase is readily estimated using a simple material balance, without any limitation on the shape of the equilibrium isotherm. The equilibrium concentration values measured in this way at $T=25$°C are shown in Fig. 2. By inspection of the resulting isotherm it is clear that the assumption of linear equilibrium is valid up to a concentration value in the fluid phase around 1.2 g dm^{-3}. Therefore, this concentration limit will never be exceeded in the rest of this work.

3.2. Column efficiency

From the same set of pulse experiments, the values of the two parameters a_i and b_i in Eq. (5) were estimated at $T=25$°C. These values are summarised in Table 4 for both sucrose and betaine. In all cases a reasonably good linearity of HETP vs. fluid velocity was verified, as is shown in Figs. 3 and 4 for the two components. Since the measured HETP values are larger for sucrose than for betaine, the first component was always considered as reference when dealing with the column length evaluation (cf. next section).

From the b values, the diffusion coefficients of both sucrose and betaine inside the polymeric particle were estimated from Eq. (4). The numerical values are reported in the same Table 4. These values compare favourably with those expected for diffusion of liquids into a microporous polymer

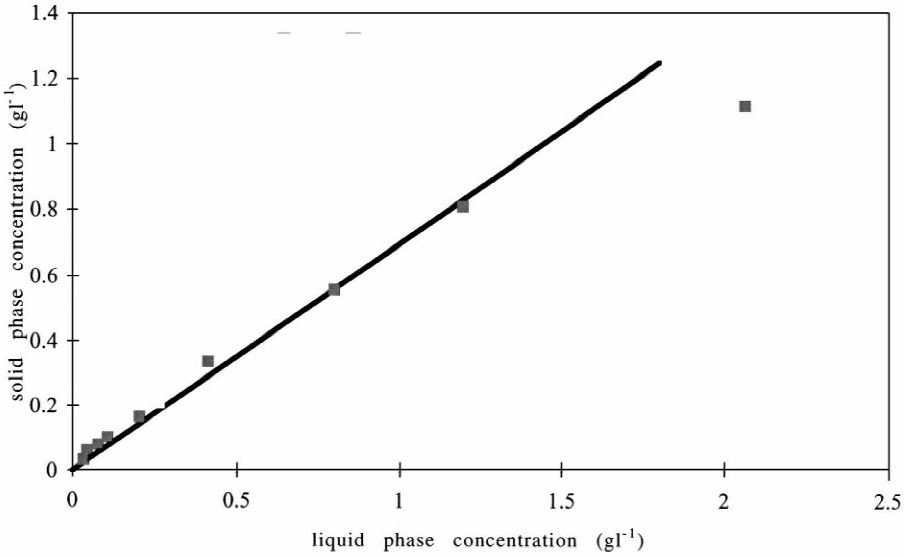

Fig. 2. Equilibrium isotherm of betaine at $T=25°C$.

Table 4
Values of the two parameters a_i and b_i in Eq. (5) and micropore diffusivity estimated at $T=25°C$

Component	a	b (s cm^{-2})	D_s (cm^2 s^{-1})
Sucrose	28.7	$1.15\cdot10^6$	$1.8\cdot10^{-8}$
Betaine	30.4	$0.66\cdot10^6$	$0.3\cdot10^{-8}$

matrix of gel type resins at similar operating conditions [14].

4. Results and discussion

The equilibrium and column efficiency data evalu-

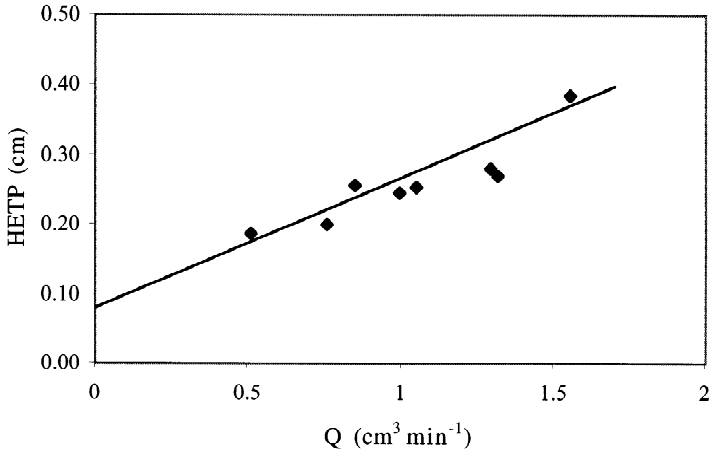

Fig. 3. HETP vs. fluid velocity for sucrose at $T=25°C$.

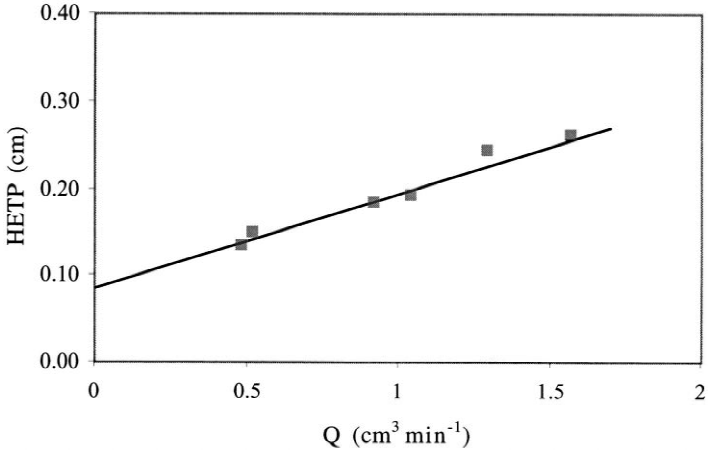

Fig. 4. HETP vs. fluid velocity for betaine at $T=25°C$.

ated by the experiments described in the previous section were used to perform a preliminary design of a SMB unit for separation of the binary mixture sucrose–betaine in diluted aqueous solution. We will consider the classical four-section configuration schematically shown in Fig. 5. According to the conventional design procedures [9,15,16], a counter-current unit (true moving bed, TMB; Fig. 5a) is first considered and the operating conditions of the equivalent SMB (Fig. 5b) are then evaluated, with the notable simplification of linear adsorption equilibria.

4.1. Identification of the separation region

In the frame of equilibrium theory (no mass transport limitations, no axial mixing), the net velocity of the ith component in section j is related to fluid and solid flow-rates by the following equation:

$$v_{cij} = \frac{u_j - u_S K_i}{\epsilon + (1-\epsilon)K_i} \quad (i = 1, 2;\ j = 1\text{–}4) \tag{9}$$

where u_j and u_S indicate the fluid and solid superficial velocity, respectively. Note that $i=1$ identifies the most adsorbable component (betaine) and $i=2$ the less adsorbable (sucrose). To assure a complete separation (complete recovery of betaine in the extract and of sucrose in the raffinate), the flow-rate ratios, u_j/u_S, have to fulfil the following inequalities [9]:

$$\text{section 1} \quad \frac{u_1}{u_S} \geq K_1 \tag{10}$$

$$\text{section 2} \quad K_2 \leq \frac{u_2}{u_S} \leq K_1 \tag{11}$$

$$\text{section 3} \quad K_2 \leq \frac{u_3}{u_S} \leq K_1 \tag{12}$$

$$\text{section 4} \quad \frac{u_4}{u_S} \leq K_2 \tag{13}$$

Since the separation is established in the two central sections of the unit, 2 and 3, all possible combinations of the admissible pairs of u_2/u_S–u_3/u_S are usually plotted to identify the so-called separation region [16]. This region, in the case of linear equilibria, is a rectangular triangle in the u_2/u_S–u_3/u_S plane. A close fulfilment of all previous inequalities (with $u_2/u_S=K_2$ and $u_3/u_S=K_1$) corresponds to ‘‘optimal’’ operating conditions, i.e., maximum feed flow-rate ratio, u_F/u_S, and minimum eluent flow-rate ratio, u_D/u_S. This ‘‘optimal’’ operating point corresponds to the vertex of the triangular separation region mentioned above.

On the other hand, it is readily understood that this operating point has no robustness to disturbances in the column flow-rates. Therefore, it does not corre-

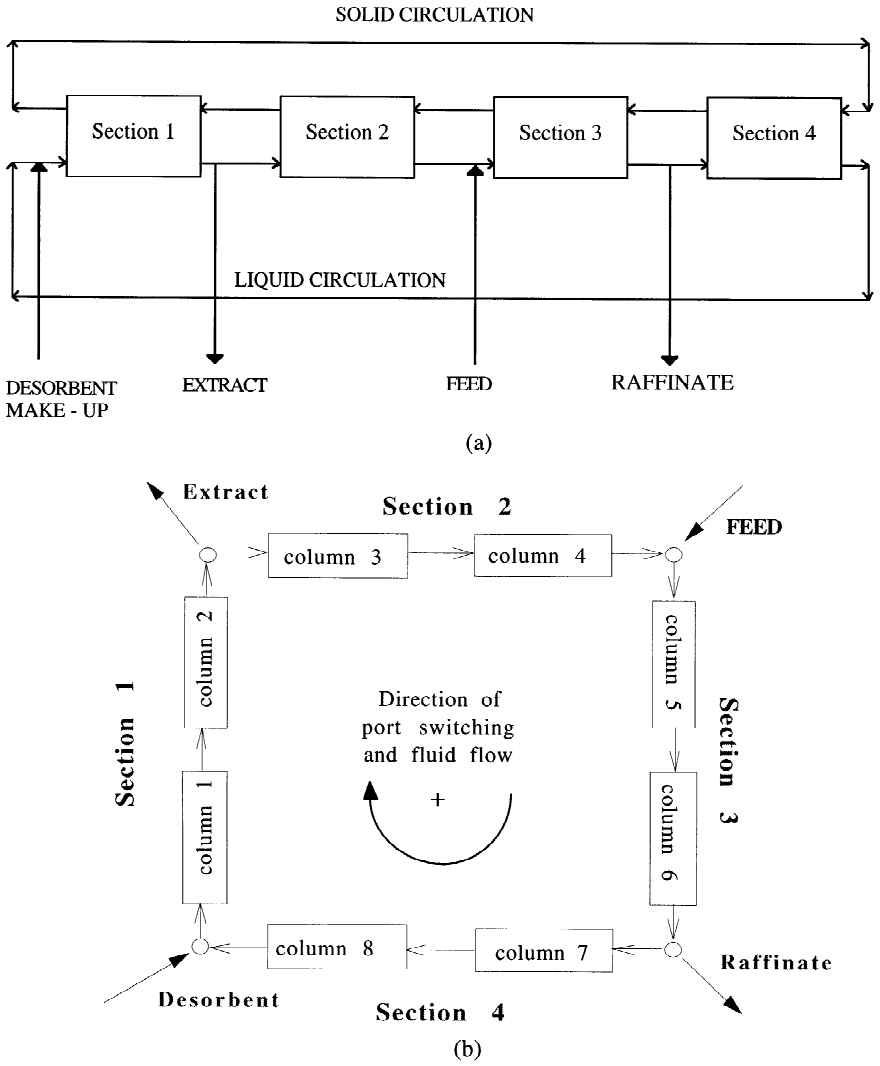

Fig. 5. Schemes of TMB (a) and SMB (b) units.

spond to the actual operating point which is usually set by introducing a correction α to the optimal values as follows:

$$\frac{u_j}{u_S} = \left(\frac{u_j}{u_S}\right)_{\text{opt}} \cdot (1+\alpha) \quad (j = 1\text{–}4) \tag{14}$$

where α has a positive value for $j=1$, 3 and the same but negative value for $j=2$, 4. In this work $\alpha=0.1$ was used.

The actual concentration values corresponding to these flow-rate ratios and equilibrium conditions (i.e., infinite column length or stage number) were evaluated by solving the following set of linear algebraic equations:

Material balance of component i in section j.

$$c_{0,ij}Q_j + q_{\text{L},ij}Q_S = q_{0,ij}Q_s + c_{\text{L},ij}Q_j \quad (i = 1, 2;\ j = 1\text{–}4) \tag{15}$$

Material balances at the section nodes.

$$\begin{aligned}
&q_{0,i1} = q_{\mathrm{L},i4} && (i = 1, 2)\\
&q_{ij} = q_{\mathrm{L},ij-1} && (i = 1, 2;\ j = 2\text{–}4)\\
&c_{\mathrm{L},i2}(K_2 + \alpha) + c_{\mathrm{F}i}(K_1 - K_2 - 2\alpha) = c_{0,i3}(K_1 - \alpha) && (i = 1, 2)\\
&c_{\mathrm{L},i4}(K_2 - \alpha) = c_{0,i1}(K_1 + \alpha) && (i = 1, 2)
\end{aligned} \tag{16}$$

Pinch conditions.

$$\begin{array}{ll}
i = 1 & i = 2\\
q_{0,i1} = Kc_{0,i1} & q_{0,i1} = Kc_{0,i1}\\
q_{\mathrm{L},i2} = Kc_{\mathrm{L},i2} & q_{0,i2} = Kc_{0,i2}\\
q_{\mathrm{L},i3} = Kc_{\mathrm{L},i3} & q_{0,i3} = Kc_{0,i3}\\
q_{\mathrm{L},i4} = Kc_{\mathrm{L},i4} & q_{\mathrm{L},i4} = Kc_{\mathrm{L},i4}
\end{array} \tag{17}$$

In the previous equations, the concentration values in the streams entering and leaving the generic section were indicated as schematically shown in Fig. 6. Note that the pinch conditions reflect the assumption of equilibrium conditions, i.e., the absence of mass transport resistances and axial mixing. Finally, it is worth mentioning that the problem can be solved independently for each component, due to the linearity of the adsorption equilibria.

To conclude, the McCabe–Thiele diagrams for both components are shown in Fig. 7a and b. The intersections between operating and equilibrium lines correspond to the pinch conditions for each component in each section (Eq. (17)).

4.2. Evaluation of the column length

Once more with reference to the TMB, the minimum number of equilibrium stages needed to obtain the desired separation has been estimated as follows. A recovery, R_i, equal to at least 99% was required for both components as separation target, being the recovery defined as the relative amount of component in the extract/raffinate with respect to the amount in the feed.

First, with separate reference to each component, the stage numbers for each section are estimated using the Kremser equation in the following form:

$$N_{ij} = \frac{\ln \dfrac{q_{\mathrm{L},ij} - q_{ij}^{\infty}}{q_{0,ij} - q_{ij}^{\infty}}}{\ln \gamma_{ij}} \quad (i = 1, 2;\ j = 1\text{–}4) \tag{18}$$

where q_{ij}^{∞} indicates the concentration value in the adsorbed phase corresponding to pinch conditions, i.e., infinite stage number and $\gamma_{ij} = u_j/(K_i u_{\mathrm{S}})$. Depending upon the actual i–j combination (cf. Eq. (17)), a constant shifting factor, β, from the corresponding pinch conditions was arbitrarily imposed. Namely, the arguments of the logarithm at numerator in Eq. (18) for all i–j combinations become:

$$\begin{array}{ll}
i = 1 & i = 2\\
(q_{1,i\mathrm{L}} - q_{1,i}^{\infty})/\beta & (q_{1,i\mathrm{L}} - q_{1,i}^{\infty})/\beta\\
\beta/(q_{2,i0} - q_{2,i}^{\infty}) & (q_{2,i\mathrm{L}} - q_{2,i}^{\infty})/\beta\\
\beta/(q_{3,i0} - q_{3,i}^{\infty}) & (q_{3,i\mathrm{L}} - q_{3,i}^{\infty})/\beta\\
\beta/(q_{4,i0} - q_{4,i}^{\infty}) & \beta/(q_{4,i0} - q_{4,i}^{\infty})
\end{array} \tag{19}$$

where the remaining values of the concentrations in adsorbed phase correspond to those calculated under the assumption of equilibrium conditions. Of course, the separation performance of the unit approaches that of the unit with infinite length (i.e., at equilib-

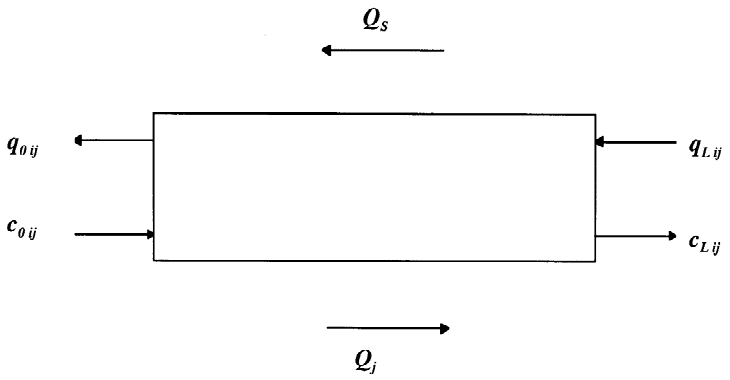

Fig. 6. Scheme of the generic counter-current section.

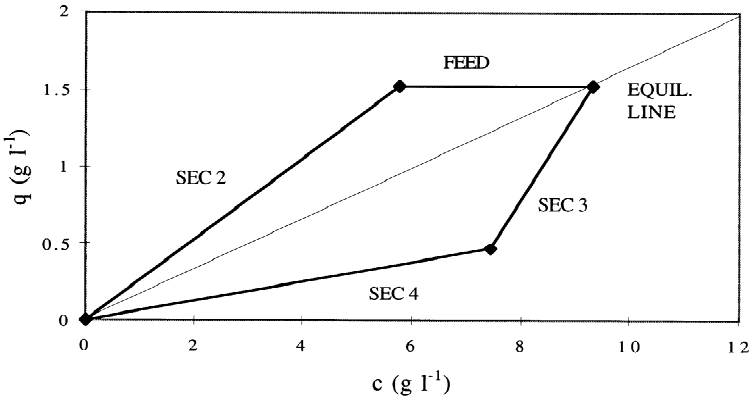

(a)

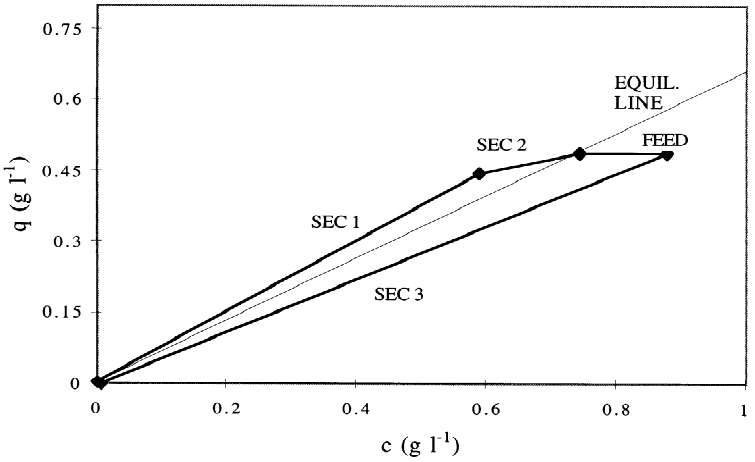

(b)

Fig. 7. McCabe–Thiele diagrams for sucrose (a) and betaine (b) of the TMB unit at infinite stage number.

rium) when β approaches 0. A pair of values of the number of stages for each section is obtained, corresponding to the two components to be separated. The actual value of the stage number for each section was selected as the maximum between these two, thus obtaining the ''configuration'' of the unit (stage number for each section).

Secondly, the separation performance of the resulting unit was evaluated using the set of equations above, (15) and (16), while replacing the pinch conditions once more using the Kremser equation (18).

The numbers of ideal stages for each section corresponding to different values of β are shown in Table 5 along with the resulting recoveries. It is readily verified that an overall number of stages $N=66$ (corresponding to $\beta=10^{-2}$ g dm^{-3}) fulfils the requirement, while for $N\geq 140$ (corresponding to $\beta=10^{-4}$ g dm^{-3}) the performance of the unit becomes practically coincident with that of the ideal one. The McCabe–Thiele diagrams at $N=66$ are almost identical to those of Fig. 7.

4.3. Selection of the SMB configuration

The values of the TMB stage numbers were used to estimate the corresponding SMB values. Since the typical number of columns (or subsections) in SMB

Table 5
Numbers of ideal stages for each section corresponding to different values of β with the resulting recoveries

β	10^{-4}	10^{-3}	10^{-2}
N_1	59.4	43.1	26.9
N_2	20.2	15.4	10.6
N_3	51.4	37.5	23.6
N_4	9.0	6.5	4.1
N	140	103	66
R_1	99.99	99.92	99.14
R_2	100.00	99.98	99.85

units is from 6 to 8, the maximum value was selected to assure a certain flexibility. Then, the unit configuration was set to fit as closely as possible the length distribution in the equivalent TMB. Namely, from the values in Table 5, the configuration 3:1:3:1 was considered, with an ideal stage number per subsection equal to 8.25.

4.4. SMB average liquid velocity and column length

Following the analysis performed by Charton and Nicoud [15], the values of subsection length, L, and average liquid velocity, v_m (defined as average of the liquid velocities in the four sections) are estimated by imposing the fulfilment of the following two inequalities:

$$\frac{L}{v_m} \geq \frac{N_{tot}}{N_c} \cdot \left(\frac{a_i r_p}{v_m} + b_i r_p^2 \right) \tag{20}$$

$$\frac{L}{v_m} \leq \frac{\Delta P_{max}}{N_c \Phi v_m^2} \tag{21}$$

The first equation is readily derived from the relationship between column length and number of ideal stages, using the expression for HETP given by Eq. (5). The second equation assures that the pressure drop in the column is below a maximum limiting value, ΔP_{max}. The parameter Φ is identified when a particular relationship for pressure drop evaluation is considered. In this work, the Blake–Kozeny equation [17] was used and the following expression applies:

$$\Phi = \frac{37.5\mu}{r_p^2} \cdot \left(\frac{1-\epsilon}{\epsilon} \right)^2 \tag{22}$$

Under operating conditions defined ‘‘laboratory unit’’ and detailed in the subsection SMB, separation performance and a maximum pressure drop $\Delta P_{max} =$ 1 bar, the calculated curves corresponding to the equalities in Eqs. (20) and (21) for the binary separation under examination are shown in Fig. 8.

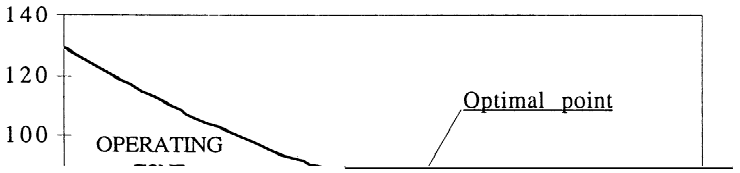

Fig. 8. Region of admissible values of the ration L/v_m.

rium non linearity), to simulate actual concentrations in beet molasses.

6. Symbols

a	Means Constant in Eq. (5)
b	Means Constant in Eq. (5) (s cm^{-2})
C_D	Means Desorbent consumption (l g^{-1})
c	Means Liquid phase concentration (g dm^{-3})
D_L	Means Axial mixing coefficient (cm^2 s^{-1})
D_S	Means Diffusion coefficient inside the particle (cm^2 s^{-1})
d_c	Means Column diameter (cm)
HETP	Means Height equivalent to a theoretical plate (cm)
K	Means Equilibrium constant of adsorption
K'	Means Capacity factor
L	Means Column length (cm)
N	Means Number of theoretical stages
Pr	Means Productivity (g dm^{-3} h^{-1})
ΔP_{max}	Means Pressure drop (bar)
Q	Means Volumetric flow-rate (l min^{-1})
q	Means Solid-phase concentration (g dm^{-3})
r_p	Means Particle radius (cm)
R	Means Separation performance
t_m	Means Characteristic time of diffusion (s)
Δt	Means Switching time (s)
u	Means Superficial velocity (cm s^{-1})
V_C	Means Column volume (cm^3)
v	Means Interstitial velocity of the fluid phase (cm s^{-1})
v_C	Means Net velocity (cm s^{-1})

Greek letters

α	Means Correction parameter in Eq. (14)
β	Means Shifting factor from pinch conditions
γ	Means Adsorption factor in Kremser equations
ϵ	Means External void fraction
μ	Means Eluent viscosity (bar s)
μ_1	Means First moment (min)
σ^2	Means Variance (min^2)
Φ	Means Parameter used in Eq. (21) (bar s^{-1} cm^{-2})

Subscripts

D	Means Refers to the desorbent
F	Means Refers to the feed
i	Means Refers to the ith component
j	Means Refers to the jth section
m	Means Refers to average conditions in the sections
S	Means Refers to the solid-phase

References

[1] H. Heikkila, Chem. Eng. 24 (1983) 50.
[2] H.A. Paananen, Zuckerind 122 (1997) 28.
[3] H. Heikkila, G. Hyoky, J. Kuisma, US Pat. No. 5 102 553 (1992).
[4] M. Munir, Sucr. Belge. Sugar Ind. 94 (1975) 333.
[5] P.E. Barker, K. Joshi, J. Chem. Tech. Biotechnol. 52 (1991) 93.
[6] S. Kishihara, S. Fujii, H. Tamaki, K.B. Kim, N. Wakiuchi, T. Yamamoto, Int. Sugar J. 94 (1992) 305.
[7] M. Saska, S.J. Clarke, M.D. Wu, K. Iqbal, Int. Sugar J. 93 (1991) 223.
[8] M. Saska, M.D. Wu, S.J. Clarke, K. Iqbal, Sep. Sci. Technol. 27 (1992) 1711.
[9] D.M. Ruthven, C.B. Ching, Chem. Eng. Sci. 44 (1989) 1011.
[10] M.D. LeVan, G. Carta, C.M. Yon, in: D.W. Green, J.O. Maloney (Eds.), Perry's Chemical Engineers' Handbook, 7th Edition, McGraw-Hill, New York, 1997.
[11] H.W. Haynes, P.N. Sarma, AIChE J. 19 (1973) 1043.
[12] J.J. Van Deemter, F.J. Zuiderweg, A. Klinkenberg, Chem. Eng. Sci. 5 (1956) 71.
[13] D.M. Ruthven, C.B. Ching, in: G. Ganetsos, P.E. Barker (Eds.), Preparative and Production Scale Chromatography, Marcel Dekker, New York, 1993.
[14] G.K. Acker, R. L Steere, Biochim. Biophys. Acta 59 (1962) 137.
[15] F. Charton, R.M. Nicoud, J. Chromatogr. A 702 (1995) 97.
[16] G. Storti, R. Baciocchi, M. Mazzotti, M. Morbidelli, Ind. Eng. Chem. Res. 34 (1995) 288.
[17] R.B. Bird, W.E. Stewart, E.N. Lightfoot, Transport Phenomena, Wiley, New York, 1960.